Open Access Library Journal
2025, Volume 12, e14123
ISSN Online: 2333-9721
ISSN Print: 2333-9705

Assessing the Relationship between Land Use/Land Cover Change, NDVI, NDBI, and Land Surface Temperature: A 20-Year Analysis of Rupandehi District, Nepal

Ashok Gahatraj[1], Keshav Raj Bhusal[2*]

[1]Department of Geography and Environmental Studies, New Mexico State University, Las Cruces, USA
[2]Department of Geomatics Engineering, Institute of Engineering, Pashchimanchal Campus, Pokhara, Nepal
Email: *hello.keshavrajbhusal@gmail.com

How to cite this paper: Gahatraj, A. and Bhusal, K.R. (2025) Assessing the Relationship between Land Use/Land Cover Change, NDVI, NDBI, and Land Surface Temperature: A 20-Year Analysis of Rupandehi District, Nepal. *Open Access Library Journal*, **12**: e14123.
https://doi.org/10.4236/oalib.1114123

Received: August 15, 2025
Accepted: September 13, 2025
Published: September 16, 2025

Abstract

This research aims to explore changes in Land Use and Land Cover (LULC) and how LULC have an influence on the Land Surface Temperature (LST) in Rupandehi district. Multiple Landsat imagery across the two decades was utilized, particularly Landsat 7 ETM+ for 2003 and 2013, and Landsat 8 OLI/TIRS for 2023. Both QGIS and ArcGIS Pro were used for spectral indexing. LULC classification was performed in R using Random Forest, where 5 major classes were categorized. A confusion matrix that was also performed in R for all the years yielded above 91% accuracy with not higher than 9% Out-Of-Bag (OOB) error rate. Categorical change detection that was performed in ArcGIS Pro revealed a significant expansion of urban areas, where larger portions were gained from agricultural and forest areas. Normalized Difference Vegetation Index (NDVI) and Normalized Difference Built-up Index (NDBI) were calculated to account for vegetation and urban features. The single-channel algorithm and thermal bands (Band 10 for Landsat 8 and Band 6 for Landsat 7) were used to compute LST. Regression analysis across the years for the NDVI and LST shows a negative correlation, while a positive correlation is observed between NDBI and LST. The outcomes of this analysis highlighted that the expansion of urban features has a substantial impact on increasing LST, which can lead to the Urban Heat Island (UHI) effect. In contrast, loss of vegetation also contributes to increasing surface temperatures. These results emphasize the importance of strategic urban planning and sustainable land management policy in the rapidly urbanizing district like Rupandehi.

Subject Areas

Geography, Geomatics Engineering, Earth & Planetary Sciences,

Environmental Science

Keywords

LULC, LST, UHI, Random Forest, Rupandehi District

1. Introduction

Land cover refers to the physical materials present on the Earth's surface, such as natural or cultivated vegetation and built structures. Land use describes how people utilize these land cover types through various activities, arrangements, and inputs to develop, modify, or sustain them [1]. Land cover has been an important variable for various studies related to food security, climate change, environmental studies, conservation strategies, hydrology, and landscape planning [2]. The studies related to LULC change provide handy information related to current LULC trends, previous practices, and future LULC trends [3] [4]. LULC changes have the potential to have a notable environmental impact, changing the urban climate [5]. Land Use Land Cover is altered dramatically by a quickly growing urban population [6]. Due to rapid urbanization and infrastructure development, most of the vegetation and farmland have been converted into urban centers, escalating the land surface temperature [7]. Land Surface Temperature (LST) is the radiative skin temperature of the land as determined by solar radiation [8]. Numerous studies found that LULC has a significant impact on surface temperature and that, particularly in metropolitan areas, LULC variation determines the relative increase in LST [9] [10]. The LST rises as a result of LULC changes, creating Urban Heat Islands (UHI), which are directly linked to high energy use, air pollution, and health hazards [11]-[13].

The LULC of urban expansion and improvement has been extensively studied in both developed and developing countries, with developing countries seeming to have more complex spatial expansion [14]. Several recent studies related to LULC change and LST have been done in South Asian countries like India [15], Bangladesh [16] and Pakistan [17]. In Nepal, research related to LULC and LST has been done in various regions, such as the Phewa Watershed [18], Kathmandu valley [19] [20] and the Central Himalayan region by ICIMOD [21]. However, a similar study has not been done for the Rupandehi district. Though [22] has done work on land cover and its impact on ecosystem services, it has rarely touched on the urban heat islands.

Rupandehi is one of the rapidly growing districts; land cover has changed a lot over the years. Rupandehi consistently falls under the top five populated districts of Nepal, where the annual population growth is 2.33% [23]. It is observed that the built-up area has been increasing over the years in Rupandehi and is centered more in Butwal and Bhairahawa cities [22]. Since Urban areas exhibit a significantly higher level of LST than other LCs, this indicates that LST can exhibit both

temporal and spatial variability [24].

Conventional studies that rely on fieldwork are costly, time-consuming, and inapplicable to large-scale investigations [25]. The combination of GIS and Remote Sensing technology is efficient in assessing, detecting, and modeling LULC and LST changes [26] [27]. Geographic Information Systems and Remote Sensing are effective tools for analyzing LULC and LST changes [28]. A lot of studies have been done to analyze the relationship between LULC and LST with GIS and Remote sensing techniques using multi-temporal Landsat imagery [29] [30]. This study analyzes the change in LULC and its effect on LST over the years 2003, 2013, and 2023, applying a GIS/Remote Sensing tool using multi-spectral Landsat 7, 8 data. Similarly, the relationships between LST, Normalized Difference Built-up Index (NDBI), and Normalized Difference Vegetation Index (NDVI) were analyzed using linear regression as done by studies like [31] [32].

This study has three major objectives: 1) To assess the spatial and temporal changes in Land Use and Land Cover (LULC) in Rupandehi District between 2003 and 2023. 2) To examine the connection between Land Surface Temperature (LST) and LULC dynamics during the study period. 3) To assess how LST and biophysical indices, such as NDVI and NDBI, correlate. LULC classification was done using Random Forest in R and raster packages. For the LST calculation, thermal bands have been used with formulas as provided in the USGS manual. This study shows how changes in land cover, especially the transition of agricultural land and forest areas to impervious surfaces, influence the surface temperatures. Rupandehi is one of the rapidly growing districts; therefore, this area is more vulnerable to climate-related stresses. The outcomes of this research will provide crucial information regarding strategic urban planning techniques to minimize the risk associated with increasing surface temperatures in Rupandehi, alongside promoting green city development.

2. Materials and Methods

2.1. Study Area

Rupandehi district comes under Lumbini province of Nepal, which is located at 27˚35'32.64" (see **Figure 1**) North longitude and 83˚26'46.68" East latitude close to the Chure range. The total area of this district is 1360 square kilometers, with an altitude ranging from 95 m to 1219 m above sea level. The highest temperature reaches up to 43.4˚C around May-June, while the minimum mean temperature of the area is 18.2˚C. The district has varied terrain, where the majority of the area is covered with plains, and some of the northern regions are covered with Chure hills. There are three major rivers in the district, namely Tinau, Danab, and Siyari, along with 289 lakes and numerous water reservoirs [33].

Siddhartha Highway and Mahendra Highway are two major roads that link Rupandehi to the country's hill and eastern-western part, respectively. The only international airport of Lumbini province, Gautam Buddha International Airport, is also located in this district. Huge areas of flat, fertile plains, plenty of monsoon

rainfall, and accessible irrigation from abundant water resources, as well as proximity to India, make this district a good place for agriculture and settlement. Rupandehi has become an economic and social hub of western Nepal, attracting lots of domestic immigrants from the hilly district and rural areas in cities like Butwal and Bhairahawa, with Tilottama. The district has consistently been the third most populous district since the census years 2001, 2011, and 2021, with population sizes of 3.06%, 3.32% and 3.86% respectively [34]. This increasing population with rapid urbanization and changing land use and land cover has made this area favorable for the study of LULC, LST, and other parameters.

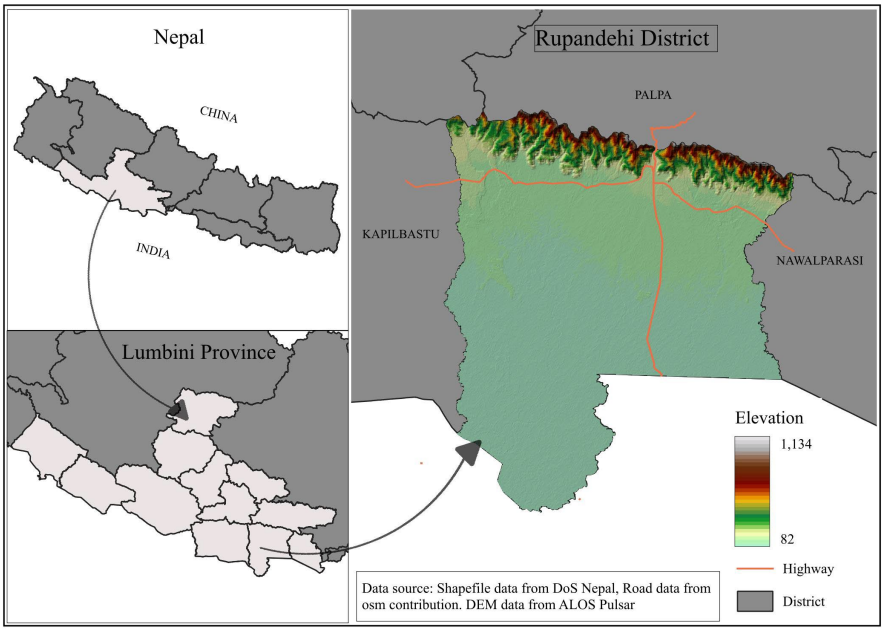

Figure 1. Map showing the study area of Rupandehi district. (Source: authors)

2.2. Dataset Required

This study has used multi-temporal satellite imagery from Landsat 7 Enhanced Thematic Mapper Plus (ETM+) and Landsat 8 Operational Land Imager (OLI). These imageries were downloaded from the United States Geological Survey (USGS) Earth Explorer website. Years 2003, 2013, and 2023 were selected to do classification across the two decadal Land Use and Land Cover (LULC) changes in Rupandehi District. To ensure temporal stability and lower phenological variability, images were acquired in the same month (March) for all three years. Cloud cover was lower compared to other months, which contributed to the desired accuracy of classification. (Table 1)

2.3. Data Processing

A series of preprocessing steps was carried out to ensure the accuracy and consistency of the satellite imagery throughout the three years. All Landsat imagery, both Landsat 8 OLI/TIRS and Landsat 7 ETM+ of respective years, was

Table 1. The details of the acquired imagery were extracted from the corresponding metadata (MTL) files.

Satellite	Year	Acquisition date	Path/Row	Resolution	Cloud Cover (%)
Landsat 7	2003	2003-03-11	142/041	30 m	0
Landsat 7	2013	2013-03-22	142/041	30 m	1
Landsat 8	2023	2023-03-10	142/041	30 m	0.24

atmospherically corrected using the Dark Object Subtraction (DOS) technique using the QGIS Semi-Automatic Classification Plugin (SCP). This technique helps to remove atmospheric haze and scattering effects. Since the downloaded images were already georeferenced to WGS 84 UTM Zone 44N, no changes were made to them, and they were kept at the default.

Landsat 7 ETM+ imagery had a scan line error because of a sensor defect in Landsat after May 2003. To remove the scanline error, the image was processed using the tool in QGIS named "Fill NoData", which calculates the missing pixel values using the neighboring pixels. Additionally, a visual inspection was done to confirm that the major land cover features were not twisted by the interpolation.

After these correction steps, images for all the years were layer-stacked, which were further clipped to the Rupandehi District. The images were combined with natural color (4, 3, 2) for Landsat 8 and (3, 2, 1) for Landsat 7 for visualization.

2.4. LST Derivation

LST was derived from the Landsat 7 ETM+ band 6_1 for the years 2003 and 2013, and for the year 2024, band 10 of Landsat 8 OLI/TIRS was used. A single-channel algorithm was applied to derive the LST for all the years, where specific parameters were utilized from MTL files. All the calculations were performed on QGIS using the Raster calculator, where the methodologies mentioned in the following articles were used [35]-[37]. LST is sensitive to vegetation phenology and surface moisture, so we used imagery acquired from the same month of the year to standardize imagery.

2.5. LST Derivation from Landsat 8 (2023)

For the year 2023, Landsat 8 thermal band 10 (TIRS) was utilized to derive the LST. The following steps were performed.

Step 1: *Top of Atmosphere* (*TOA*) *Spectral Radiance*

$$L_\lambda = M_L \times Q_{cal} + A_L$$

where:

L_λ = TOA spectral radiance, Q_{cal} = Digital Number of Band 10

M_L = 0.00003342 (RADIANCE_MULT_BAND_10),

A_L = 0.1 (RADIANCE_ADD_BAND_10)

Step 2: *Brightness Temperature* (*in Kelvin*)

$$BT = K_2/\{\ln(K_1/L_\lambda) + 1\}$$

where:

$K_1 = 774.8853$, $K_2 = 1321.0789$, BT = Brightness Temperature (Kelvin)

Step 3: *NDVI Calculation*

$$NDVI = (NIR - Red)/(NIR + Red)$$

where:

NIR = Band 5, Red = Band 4 (All bands atmospherically corrected)

Step 4: *Proportion of Vegetation* (P_v) [38]

$$P_v = \{(NDVI - NDVI_{min})/(NDVI_{max} - NDVI_{min})\}^2$$

where $NDVI_{min}$ and $NDVI_{max}$ are the lowest and highest NDVI values of the study area, which were extracted from the image histogram, considering standard practice [39].

Step 5: *Land Surface Emissivity* (ε) [40]

$$\varepsilon = 0.004*P_v + 0.986$$

The LST output value is more affected, especially by daytime than nighttime, with the uncertainties in parameters like $NDVI_{min}$, $NDVI_{max}$, and land surface emissivity [41] so great care was given to derive these values.

Step 6: *Final LST Calculation* (*in* ˚C)

$$LST(^\circ C) = [BT/\{1 + (\lambda*BT/\rho) + *\ln(\varepsilon)\}] - 273.15$$

where:

λ = 10.895 μm (wavelength of Band 10), ρ = 14380 (constant).

2.6. LST Derivation from Landsat 7 ETM+ (2003 & 2013)

To derive the LST from Landsat 7 ETM+, thermal band 6 was used. The following steps were followed:

Step 1: *TOA Radiance Conversion*

$$L_\lambda = ((L_{MAX} - L_{MIN})/(QCAL_{MAX} - QCAL_{MIN})) \times (DN - QCAL_{MIN}) + L_{MIN}$$

where,

L_{MAX}, L_{MIN} = Maximum and minimum spectral radiance (from MTL file)

$QCAL_{MAX}$ – $QCAL_{MIN}$ = Maximum and minimum quantized calibrated pixel values (commonly 255 and 1)

Step 2*: Brightness Temperature* (*LST in* ˚C)

$$LST(^\circ C) = \{K_2/(\ln((K_1/L_\lambda) + 1)\} - 273.15$$

where,

K_1, K_2 = Calibration constants from the MTL file (typical values: K_1 = 666.09, K_2 = 1282.71).

2.7. Spectral Index Computation (NDVI and NDBI)

Two spectral indices were calculated from corrected imagery to analyze the vegetation cover and built-up area distribution over time.

The Normalized Difference Vegetation Index (NDVI) is one of the most commonly used vegetation indicators [42]. This index is calculated using the Near Infrared (NIR) and red bands. For the year 2023, Bands 5 and 4 of Landsat 8 were used, whereas for years 2003 and 2013, Bands 4 and 3 were used.

$$NDVI = (NIR - Red)/(NIR + Red)$$

To identify how built-up areas and urban sprawl occur, the Normalized Difference Built-up Index (NDBI) was calculated using the Shortwave Infrared (SWIR) and Near Infrared (NIR) bands [43]. Band 6 (SWIR) and Band 5 (NIR) were used for the year 2023, while for the years 2003 and 2013, Band 5 and Band 4 of Landsat 7 were utilized.

$$NDBI = (SWIR - NIR)/(SWIR + NIR)$$

2.8. Land Use Land Cover (LULC) Classification

Land Use and Land Cover (LULC) classification was done using the Landsat imagery directly downloaded from the USGS Earth Explorer for all three years, 2003, 2013, and 2023. LULC classification was carried out in R using the Random Forest (RF) algorithm and raster packages. RF is one of the most used ensemble learning approaches that performs with high accuracy and tackles high-dimensional remote sensing data [44].

All the imagery that was preprocessed and layer-stacked was loaded into R. Training samples were selected in QGIS and loaded into R as a shapefile. Five major classes were defined for this classification: agricultural land, built-up land, forest, barren land, and water bodies. In total, approximately 350 - 500 training samples were selected for each year, whereas for each class, 60 - 100 training samples were selected based on the spatial variability of the land. To capture the spatial heterogeneity, training samples were stratified across the district. Due to its ensemble-based learning, the Random Forest algorithm has been shown to yield robust and consistent results, even when trained on as few as 50 samples per class [45].

The labeled samples were used in a Random Forest model, where 600 trees were configured in the model. This model was then applied to classify the LULC map for each year. A confusion matrix was generated for each year to calculate the accuracy of the LULC classification. Statistics like overall accuracy, user's accuracy, and kappa coefficients were calculated for each year. Furthermore, the Out-Of-Bag (OOB) error rate is an internal cross-validation technique intrinsic to Random Forest [46].

2.9. Change Detection Analysis

Change detection for Land Use and Land Cover (LULC) was performed in ArcGIS Pro, using a categorical change detection method. The categorical change detection method contrasts raster imagery of two distinct periods, comparing each pixel to identify transitions in land cover classes [47].

In the change detection wizard, classified maps that were generated from a random forest in R were used to generate change detection for two time frames: 2003 to 2013 and 2013 to 2023. After running the categorical change tool in ArcGIS Pro, it produced a change map and transition table for each class. That land cover transition table was later used to evaluate changes in area for each class. The identification of precise land cover transformation, from agricultural to built-up and forest to barren land, was easily noticeable from the map and the conversion table, which allows for the quantification of net gain and loss of each land cover. Furthermore, change detection output highlighted major land cover conversion and spatial trends like urban expansion and deforestation areas. These statistics and spatial maps, together with NDVI, NDBI, and LST, were used to interpret the results and discussion in the Results and Discussion part. Figure 2 shows the working flow diagram of this study.

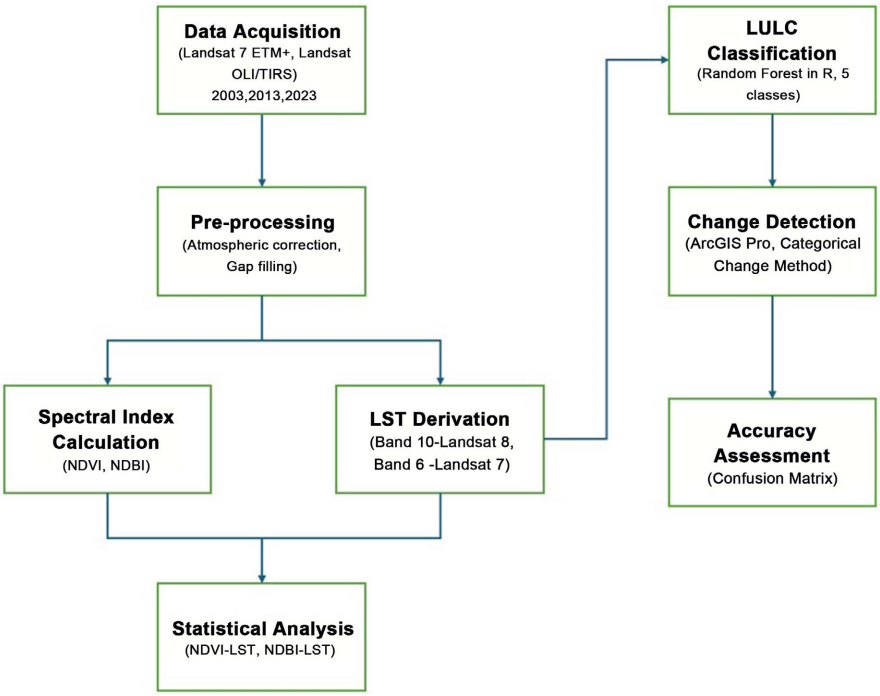

Figure 2. Workflow of the methodology used in this study.

3. Results and Discussion

3.1. Land Use Land Cover

The Land Use and Land Cover (LULC) maps of the Rupandehi District for 2 decades, from 2003 to 2023 (Figures 3-5), reveal a clear pattern of urban expansion and land transformation around the study area. The district was primarily dominated by a vast stretch of continuous agricultural land from the central and southern parts. Overall, 942.14 km^2 or 69.28% of the area was covered by agricultural land. In the northern region of the district, dense forest largely covered the area, specifically along the Siwalik Hills. In total, the forest area accounted for 23.99%

or 326.34 km^2 of the whole area. At that time, built-up areas were sparsely populated, mostly concentrated in core urban centers like Butwal and Bhairahawa, covering 42.38 km^2 (3.12%). Similarly, barren land covered 36.33 km^2 (2.67%) in total, while 12.81 km^2 (0.94%) were water bodies.

By 2013, a noticeable shift began to emerge. Looking at Table 2, the built-up area had expanded by more than double in 10 years from 2003 to 2013, reaching 97.12 km^2 (7.14%) and expanding outward mostly along the roadways and rivers around Butwal and the Bhairahawa corridor. The spread of urban areas caused adjacent agricultural land to decrease slightly to 930.99 km^2 (68.46%). Similarly, the forest area also showed a minimal decrease in area to 297.48 km^2 (21.87%). In the LULC 2013 map forest area seems still similar to what was observed in the year 2003, but some of the areas that were close to the urban centers seem fragmented. The LULC map of 2013 shows more blue colored areas in the central portion of the district, which represents an upward trend in the water bodies (16.05 km^2). Barren, on the other hand, declined to 18.34 km^2 (1.35%), possibly suggesting urban sprawl close to the riverbank. (See Figure 6)

Coming towards the end of 2023, the built-up area expanded significantly up to 218.57 km^2 (16.07%), suggesting a fivefold increase in comparison to 2003. With this vast urban sprawl, large portions of agricultural land are consumed, resulting in a reduction of 736.00 km^2 (54.12%). Looking at the LUCL map of 2023, urban expansion occurred throughout the district but mostly concentrated on the East-West highway and the Butwal and Bhairahawa corridor. Interestingly, the forest area increased to 365.96 km^2 (26.91%); the major reason behind this could be afforestation and conservation practices. Water bodies are continuously showing an upward trend (26.01 km^2, 1.91%), mostly around the central portion of the district; meanwhile, barren land continued to shrink, but by a fraction, to 13.46 km^2 (0.99%).

Both the maps and statistical tables, and the graphs indicate that a strong urban sprawl in the Rupandehi District, which was primarily an agrarian district in 2003, but in the next two decades landscape changed to a more urbanized one. These findings are supported by both the statistical table and the graphs. Table 2 provides a comprehensive overview of land transformation, while maps showcase the visuals of land use and land cover changes.

Table 2. Land use and land cover area statistics for Rupandehi District (2003, 2013, and 2023).

Class	Area 2003 (Sq·km)	2003%	Area 2013 (Sq·km)	2013%	Area 2023 (Sq·km)	2023%
Agricultural Land	942.14	69.28	930.99	68.46	736.00	54.12
Built-up Land	42.38	3.12	97.12	7.14	218.57	16.07
Barren Land	36.33	2.67	18.34	1.35	13.46	0.99
Forest	326.34	23.99	297.48	21.87	365.96	26.91
Water Bodies	12.81	0.94	16.05	1.18	26.01	1.91

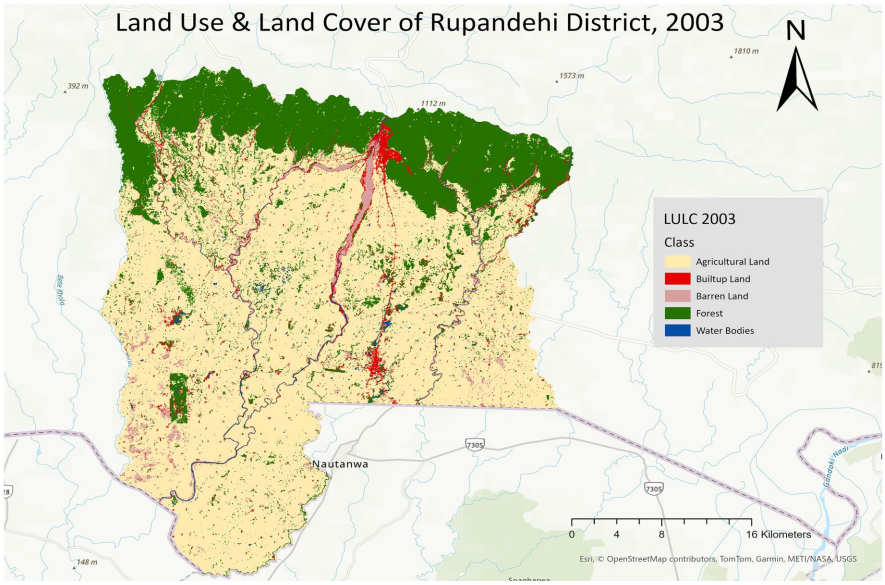

Figure 3. Land Use and Land Cover maps of Rupandehi District for the year 2003. (Source: authors)

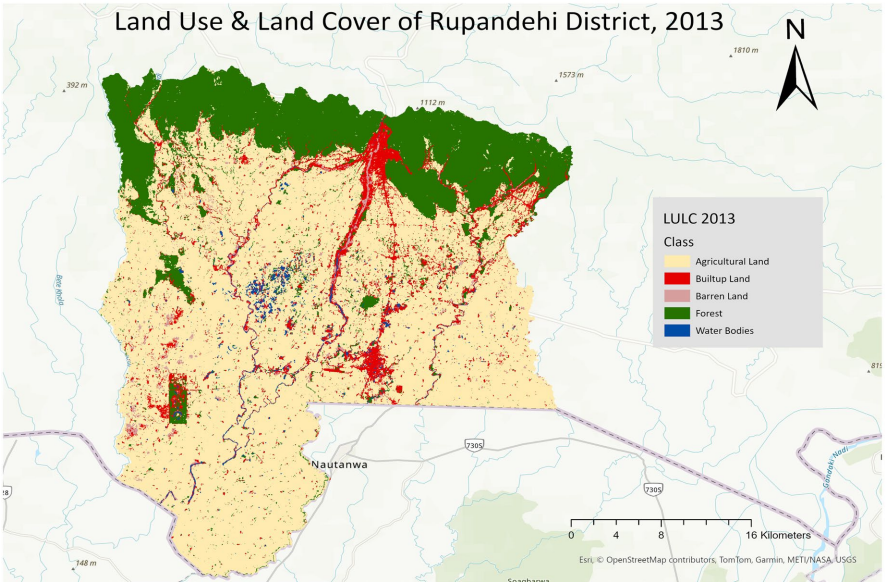

Figure 4. Land Use and Land Cover maps of Rupandehi District for the year 2013. (Source: authors)

3.2. Land Use and Land Cover Change Detection (2003-2023)

The change detection analysis reveals a dynamic transition in land use, where urban transformation became the most noticeable between 2003-2013, and 2013-2023. Analyzing land cover transitions, along with land use change matrices for each class, demonstrates the scale and direction of land conversion in the district.

During the year from 2003 to 2013, the most prominent change was from forest to agricultural land, with 31.42 km^2 of forest area transformed into agricultural land (Table 3). At the same time, 23.59 km^2 of forest area was transformed into

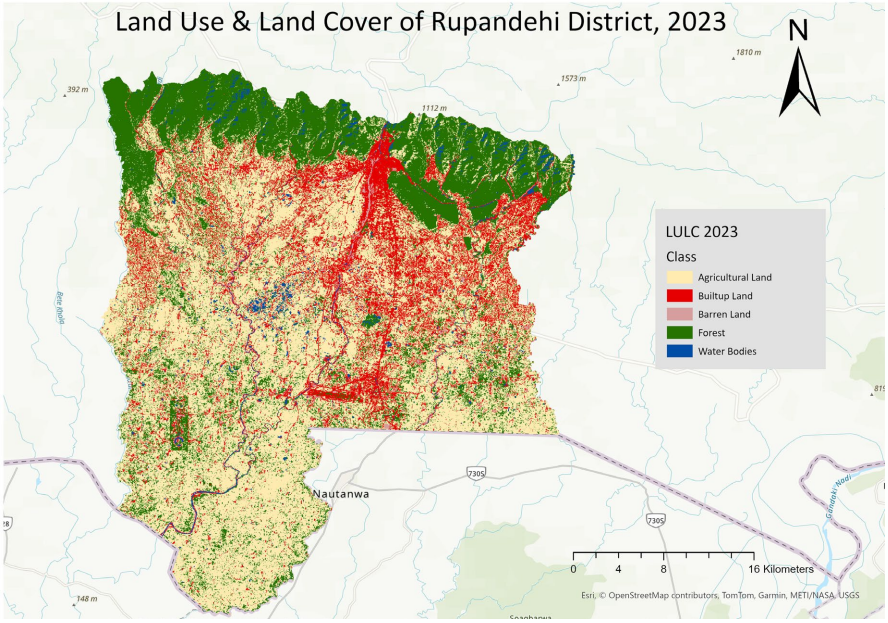

Figure 5. Land Use and Land Cover maps of Rupandehi District for the year 2023. (Source: authors)

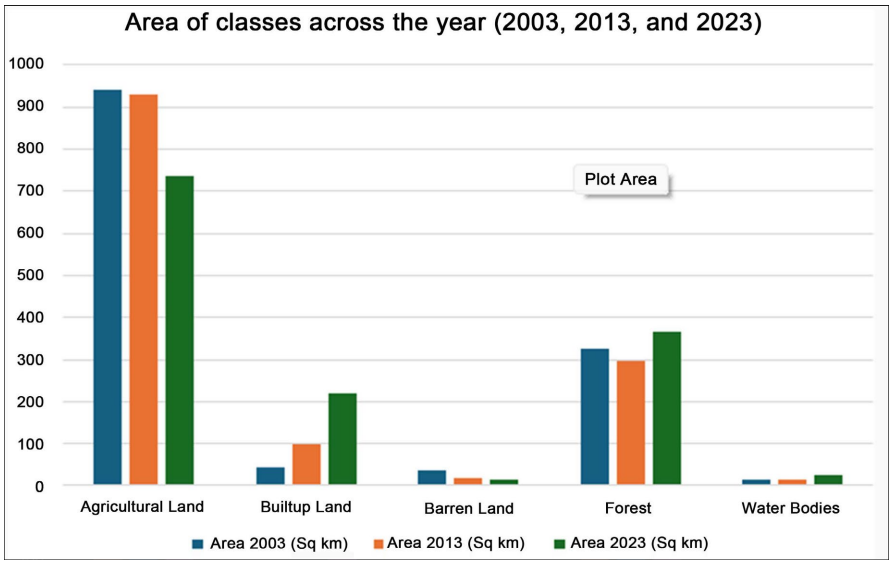

Figure 6. Bar chart showing the area (in square kilometers) of each LULC class across 2003, 2013, and 2023.

built-up area, which was likely to occur due to urban development around the Butwal and Siddhartha Nagar area. 13.53 km^2 of the farmland was lost to barren areas, which could be either because of soil degradation or loss of fertility of uncultivated land. In this period, the built-up area expanded by 17.61 km^2, gaining from agricultural areas and 15.96 km^2 from barren areas. Water bodies also gained some areas in that duration, 5.43 km^2 from the arable land, which suggests some development in irrigation infrastructure. Between 2003 and 2013, 1201.30 km^2 of land remained unchanged, while roughly 12% of the district area underwent trans-

formation.

In the next decade (2013-2023), land cover change intensity and pace continued to be more substantial. Transition from the agricultural area to built-up land, in total 102.13 km^2, was the largest, nearly Rupandehi had seen three times the urban growth as in the previous decade. Figure 7 clearly shows this transition with the dense purple zones, particularly in Butwal, Tilottama, Bhairahawa, and some new emerging towns alongside the major highways. Interestingly, forest land gained 93.36 km^2 of the area from the agricultural land, which suggests either conservation practices or reclassification of fallow fields. Around 7.65 km^2 of arable land was converted into water bodies, and 6.22 km^2 into barren land. These changes altogether highlight that agricultural land was the most vulnerable land type in Rupandehi district. (See Figure 8)

Urban area gained a noticeable amount of land from the other classes, like 24.40 km^2 from barren land, 14.31 km^2 of the forest area, and also changed to built-up land, and 3.74 km^2 of water bodies converted to built-up area. This combined transition exhibits the aggressive nature of urban encroachment into all kinds of land classes. During this period, nearly 26% of the district land experienced transformation, meaning 1005.41 km^2 of the land remained unchanged between 2013 and 2023.

In summary, the spatial change map and tabulated data highlighted that between 2003 and 2023, there was a moderate change, which includes gradual urban expansion mostly concentrated in the urban centers. On the contrary, the following decade experienced more intense and clustered transitions, particularly urban expansion in the form of some new emerging towns, agricultural fragmentation, and forest alternation. These changes not only suggest expansion of built-up areas around the major cities of the district, but also indicate urban sprawl in the whole district.

Table 3. Land cover transitions in Rupandehi District between 2003-2013 and 2013-2023 (in square kilometers).

Transition	Area 2003-2013 (km^2)	Area 2013-2023 (km^2)
Agricultural Land-> Built-up Land	17.60954	102.1321672
Agricultural Land-> Barren Land	5.63565	6.215077341
Agricultural Land-> Forest	18.82065	93.35772082
Agricultural Land-> Water Bodies	5.427579	7.645450192
Built-up Land-> Agricultural Land	3.203177	24.40217951
Built-up Land-> Barren Land	1.177515	3.161189315
Built-up Land-> Forest	2.193612	14.31119295
Built-up Land-> Water Bodies	1.265222	3.74808072
Barren Land-> Agricultural Land	13.53396	7.77607785
Barren Land-> Built-up Land	15.9599	9.369735273
Barren Land-> Forest	1.181247	1.800795566
Barren Land-> Water Bodies	1.077678	0.78656511
Forest-> Agricultural Land	31.41782	43.43183006

Continued

Forest-> Built-up Land	23.58576	11.8880499
Forest-> Barren Land	1.167251	0.742711539
Forest-> Water Bodies	4.404951	9.286693405
Water Bodies-> Agricultural Land	3.492424	6.861684246
Water Bodies-> Built-up Land	5.383726	4.096110122
Water Bodies-> Barren Land	0.682063	0.732447938
Water Bodies-> Forest	1.478892	2.842084609
No Change	1201.301	1005.412156

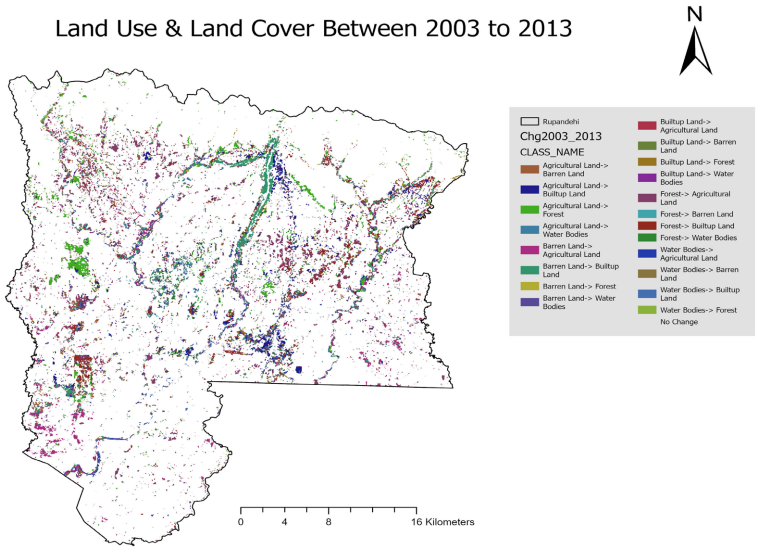

Figure 7. Land Use and Land Cover change detection maps of Rupandehi District between 2003-2013. (Source: authors)

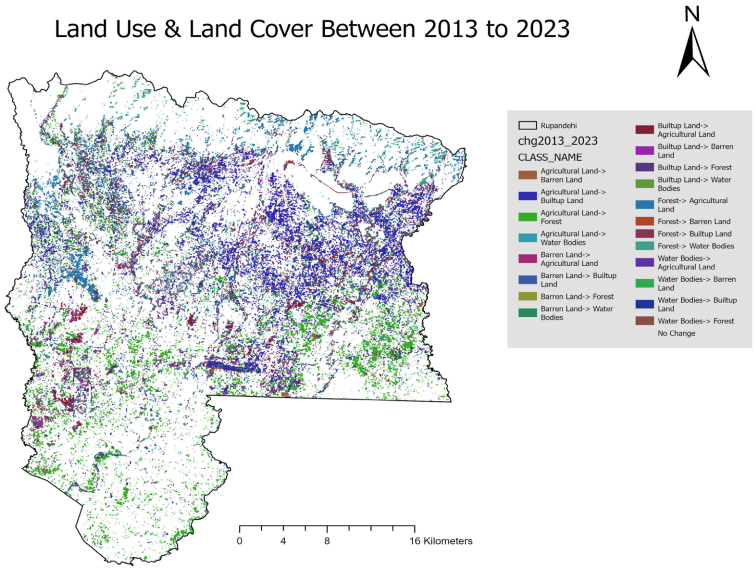

Figure 8. Land Use and Land Cover change detection maps of Rupandehi District between 2013-2023. (Source: authors)

3.3. Classification Accuracy Assessment

Out-Of-Bag (OOB) error estimates and confusion matrices were used to evaluate the accuracy of the LULC classifications for the years 2003, 2013, and 2023. A random forest classifier was used to derive the LULC classifications and error matrices. As per the accuracy assessment result, in 2003, the OOB error rate was 8.36% in total, which comes to approximately 91.64% of overall accuracy. Among all the land cover classes, built-up shows some confusion; besides that, all the classes were identified with high precision. Particularly, 9 occasions, barren land, and 5 times forest were misidentified, contributing to a high-class error of 22.06% for built-up land. In general, other classes like agricultural land (4.12%), water bodies (5.56%), and forest (4.0%) excelled in classification.

Interestingly, the LULC classification accuracy of the year 2013 was highest among the three years, where the OOB error rate was just 4.45%. This year, the random forest algorithm worked exceptionally well, resulting in low class-wise errors, specifically, the forest with 2.2%, 2.82% in barren land, 4.23% in water bodies, and 5.78% in agricultural land. Though Built-up land showed a little bit of confusion in identifying both barren and forest classes, it was still able to achieve a class error of 6.32%. In comparison 2023 OOB error was slightly higher than the previous decade but still succeeded in achieving an accuracy of 91.61%. Surprisingly, the algorithm was able to identify the built-up area more accurately than in the previous two years, with an error of 6.06% only. 14 pixels of forest were misclassified as agricultural land, which contributed to a higher error for the forest class (14.74%). Similarly, agricultural land also showed a moderate decrease in classification effectiveness, with a class error of 12.24%, which is primarily due to overlap with forest. Barren land and water bodies also continued to be well-classified with a class error of 4.11% and 2.63% respectively.

On the whole, the classification accuracy achieved from the random forest was acceptable for all the years for LULC classification. There was a slight decrease in accuracy in 2023 as compared to 2013, which could be a reflection of confusion in the spectral value in transition zones. Particularly, forest-agriculture confusion was one of the dominant reasons for slightly lower accuracy in later years. (Table 4 and Table 5)

Table 4. Confusion matrices and OOB error estimates for 2003 LULC classifications in Rupandehi District.

	Agricultural Land	Built-up Land	Barren Land	Forest	Water Bodies	Class.Error
Agricultural Land	93	2	0	1	1	0.04123711
Built-up Land	0	53	9	5	1	0.22058824
Barren Land	2	4	58	0	0	0.09375
Forest	3	1	0	96	0	0.04
Water Bodies	0	2	1	0	51	0.05555556
OOB estimate of error rate	8.36%					

Table 5. Confusion matrices and OOB error estimates for 2013 LULC classifications in Rupandehi District.

	Agricultural Land	Built-up Land	Barren Land	Forest	Water Bodies	Class.Error
Agricultural Land	114	3	1	3	0	0.05785124
Built-up Land	1	89	2	2	1	0.06315789
Barren Land	0	2	69	0	0	0.02816901
Forest	2	0	0	89	0	0.02197802
Water Bodies	0	3	0	0	68	0.04225352
OOB estimate of error rate	4.45%					

Table 6. Confusion matrices and OOB error estimates for 2023 LULC classifications in Rupandehi District.

	Agricultural Land	Built-up Land	Barren Land	Forest	Water Bodies	Class.Error
Agricultural Land	86	3	0	9	0	0.05785124
Built-up Land	1	93	4	1	0	0.06315789
Barren Land	0	3	74	0	0	0.02816901
Forest	14	0	0	81	0	0.02197802
Water Bodies	0	2	0	0	74	0.04225352
OOB estimate of error rate	8.39%					

3.4. Relationship between Vegetation, Built-Up Areas, and Land Surface Temperature

To understand the impact of the vegetation and built-up areas on the Land Surface Temperature (LST), linear regression analyses were conducted for the years 2003, 2013, and 2023, correlating LST with both NDVI as a vegetation metric and NDBI as a built-up metric. Both regression analyses supported the urban sprawl pattern in the Rupandehi district, which was noted in LULC classification, where the regression line manifests strong and predictable trends.

In all three years, a strong negative correlation was noticed between LST and NDVI, which affirms that a higher concentration of vegetation leads to lower land surface temperature, because of cooling effects like evapotranspiration and shading. R^2 value of 0.34 was observed for NDVI-LST in 2003, with the regression equation $Y = -8.78X + 23.79$, which indicates a modest opposite trend. In the year 2013, the relationship became slightly stronger, reaching $R^2 = 0.43$ and a steeper slope ($Y = -16.65X + 29.48$). This highlights the increasing influence of vegetation as a cooling agent while urban areas continue to grow. The correlation value dropped slightly in the year 2023 ($R^2 = 0.32$), which could have been caused by more land cover fragmentation and spectral mixing in peri-urban areas.

On the other hand, the NDBI (built-up index) and the LST interrelationship were positive and strong for all three years. This correlation highlights that urban infrastructure contributed a significant portion to the land surface heating. In the year 2003, the regression analysis indicated a noticeable contribution of impervious surfaces to retaining heat, where the R^2 value was 0.53 and the slope was 9.6.

The contribution of urban infrastructure to the land surface temperature intensified more in 2003 than in the previous decade, which was clearly supported by the regression analysis, where $R^2 = 0.68$ and $Y = 15.99X + 26.87$. In 2023, the strong relationship continued ($R^2 = 0.54$, $Y = 22.32X + 30.34$), supporting that urban features were determinant in retaining heat.

These regression analysis results clearly support the land cover change patterns that were observed from random forest classification, illustrating that when vegetation is replaced by impervious surfaces, the capacity to retain heat by the land increases. The regression analysis parameters, both the R^2 value and the slope across the 3 years, demonstrated that the influence of vegetation on the cooling and heating of impervious surfaces has become equally prominent over time. (See Figure 9 and Figure 10)

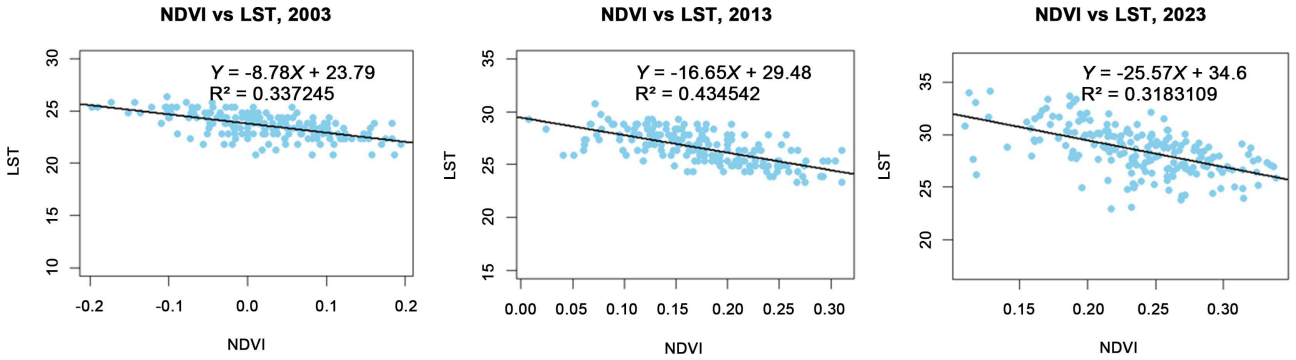

Figure 9. NDVI vs Land Surface Temperature (LST) Regression Plots (2003, 2013, 2023).

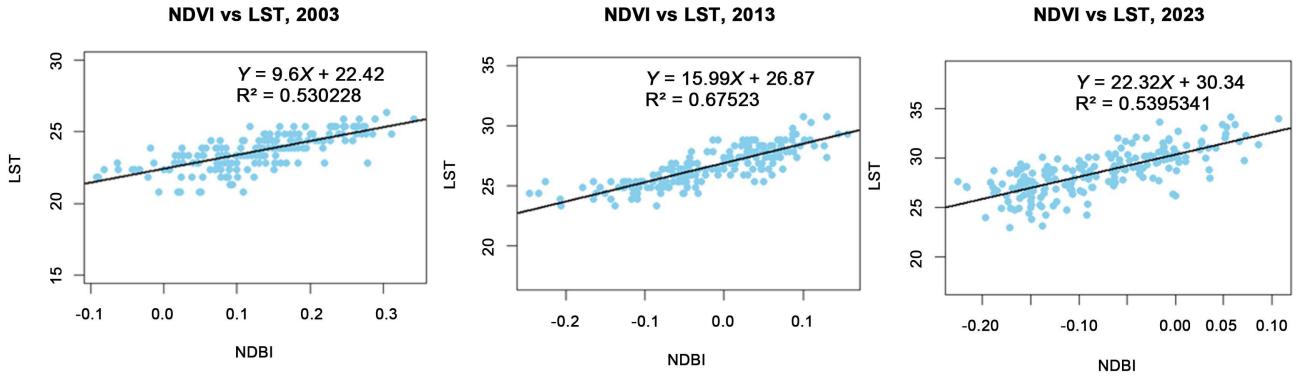

Figure 10. NDBI vs Land Surface Temperature (LST) Regression Plots (2003, 2013, 2023).

3.5. Discussion

This study's findings show a clear pattern of land transition in Rupandehi District over two decades (2003-2023). This transformation was prominently supported by rapid urban growth, which also led to a change in environmental conditions. In Nepal, the Terai district, which includes major cities like Butwal, has seen significant changes in the landscape due to rapid migration from neighboring hilly districts in the search for education, agriculture, health, and convenience [48]. The steady growth in the urban landscape and decreasing agricultural areas show that

the district is transforming into a more urbanized area, which was primarily an agrarian territory. A similar trend was observed in other rapidly growing urban zones of Nepal, where infrastructure and impervious surface development changed the peri-urban landscape [49] [50].

The most noticeable change that occurred in the transitional zone was a loss of arable land, which occurred along the major highways and in close proximity to Butwal, Tilottama, and Bhairahawa. Corridor-based urbanization pattern is very common in Nepal because they provide easy accessibility, transport infrastructure, and usually connects marketable centers with nearby residential and rural areas [51]. Similarly, the regression analysis between NDBI and LST has pointed out that growth in built-up land has contributed to increasing Land surface temperature. The findings documented in this study are consistent with the urban heat island effect, which is a well-documented and studied effect [52] [53]. In comparison to other surfaces like vegetation, barren land, water bodies, etc., impervious surfaces such as concrete and asphalt are more capable of holding heat [54].

In contrast, vegetation exhibits an opposite relation to surface temperature across the study timeline, where the correlation plot has shown an inverse relationship between NDVI and LST. This similar pattern has been studied throughout the major cities of Nepal, like Kathmandu and Pokhara [55] [56]. During the first decade of this study, the forest area was in a declining trend; interestingly, it exhibited a sign of recovery in the later years. This effect is a result of conservation practices and restoration programs initiated throughout Nepal, where environmental protection programs, such as a participatory approach, have reclaimed a larger portion of the country's forest area [57].

Agricultural land was the most vulnerable land cover class, consistently transitioning into built-up land or returning to forest. This high degree of land instability is a result of two major factors: land demand because of urban growth, and marginal agricultural yields, which are observed across the Terai zone [58]. Long-term food security, uncontrolled and chaotic urban growth, and intense UHI in urban centers are some of the potential risks that could arise because of these changes [59]. The moderate yet noticeable growth of water bodies, somewhat through the transformation of agricultural land, could be related to the development of irrigation infrastructure and pond construction for fisheries [60].

However, selecting only the March scenes was one of the limitations of this study. These results show that LST patterns showcase late dry-season conditions instead of the whole annual cycle. Furthermore, considering only one month of data limits the seasonal pattern of phenology and the temperature, since vegetation-temperature coupling may differ in the monsoon and the winter period. Even though gap-filling in Landsat 7 ETM+ was corrected, it may still introduce inaccuracies. To ensure the reliability of our findings, we lowered these effects by not including the filled areas for the training samples and also inspected the area visually.

The collective evidence, both spatially and statistically, suggests a strong relationship between land cover transformation and thermal dynamics. This finding emphasizes the need for urban planners to incorporate environmental indicators into urban and regional planning strategies. Failing to incorporate policies like green zoning, infrastructure, and vegetation preservation could worsen ecological stress and urban heat island effects [61]. This would make the district, precisely the urban centers, more vulnerable to extreme climate events.

4. Conclusions

This study analyzed two decades of land use changes in Rupandehi District (2003-2023) to understand their influence on vegetation, urban expansion, and Land Surface Temperature (LST). The outcome of the study indicated that built-up areas have increased by more than five times in two decades, mainly by replacing agricultural land. The urban sprawl was clustered around the major towns of the district, like Butwal, Bhairahawa, and major road networks. The regression analysis of NDVI-LST suggested that vegetation and land surface temperatures are positively correlated, where vegetation helps to lower the surface temperature. Similarly, NDBI-LST regression analysis shows that an increase in impervious surfaces intensifies land surface temperature, amplifying urban heat island effects.

The random forest classification that is used for land use and land cover classification has achieved more than 91% accuracy, ensuring the validity of these findings. The findings of this study suggested the need for green infrastructure and strategic land use planning to combat rising land surface temperatures and maintain ecological balance. Future research should focus on implementing socio-economic data, predictive models for future land cover scenarios, and exploring the impacts of climate variability to guide sustainable land use planning and climate adaptation strategies.

Conflicts of Interest

The authors declare no conflicts of interest.

References

[1] Food and Agriculture Organization of the United Nations (n.d.) Geospatial Information for Sustainable Food Systems. Land Cover and Land Use. https://www.fao.org/geospatial/our-work/what-we-do/land-cover-and-land-use/en/

[2] Bununu, Y.A., Bello, A. and Ahmed, A. (2023) Land Cover, Land Use, Climate Change and Food Security. *Sustainable Earth Reviews*, **6**, Article No. 16. https://doi.org/10.1186/s42055-023-00065-4

[3] Almazroui, M., Mashat, A., Assiri, M.E. and Butt, M.J. (2017) Application of Landsat Data for Urban Growth Monitoring in Jeddah. *Earth Systems and Environment*, **1**, Article No. 25. https://doi.org/10.1007/s41748-017-0028-4

[4] Bhagyanagar, R., Kawal, B.M., Dwarakish, G.S. and Surathkal, S. (2012) Land Use/Land Cover Change and Urban Expansion during 1983-2008 in the Coastal Area of Dakshina Kannada District, South India. *Journal of Applied Remote Sensing*, **6**,

Article ID: 063576-1. https://doi.org/10.1117/1.jrs.6.063576

[5] Mubeen, K. and Jabran, K. (2019) Alternate Wetting and Drying System for Water Management in Rice. In: Hasanuzzaman, M., Ed., *Agronomic Crops*, Springer, 101-110.

[6] Sminkey, P.V. and LeDoux, J. (2016) Case Management Ethics: High Professional Standards for Health Care's Interconnected Worlds. *Professional Case Management*, **21**, 193-198. https://doi.org/10.1097/ncm.0000000000000166

[7] Moisa, M.B., Dejene, I.N., Roba, Z.R. and Gemeda, D.O. (2022) Impact of Urban Land Use and Land Cover Change on Urban Heat Island and Urban Thermal Comfort Level: A Case Study of Addis Ababa City, Ethiopia. *Environmental Monitoring and Assessment*, **194**, Article No. 736. https://doi.org/10.1007/s10661-022-10414-z

[8] Jaber, S.M. (2019) On the Relationship between Normalized Difference Vegetation Index and Land Surface Temperature: MODIS-Based Analysis in a Semi-Arid to Arid Environment. *Geocarto International*, **36**, 1117-1135. https://doi.org/10.1080/10106049.2019.1633421

[9] Pal, S. and Ziaul, S. (2017) Detection of Land Use and Land Cover Change and Land Surface Temperature in English Bazar Urban Centre. *The Egyptian Journal of Remote Sensing and Space Sciences*, **20**, 125-145. https://doi.org/10.1016/j.ejrs.2016.11.003

[10] Patel, S., Indraganti, M. and Jawarneh, R.N. (2024) A Comprehensive Systematic Review: Impact of Land Use/Land Cover (LULC) on Land Surface Temperatures (LST) and Outdoor Thermal Comfort. *Building and Environment*, **249**, Article ID: 111130. https://doi.org/10.1016/j.buildenv.2023.111130

[11] Ahmed, B., Kamruzzaman, M., Zhu, X., Rahman, M. and Choi, K. (2013) Simulating Land Cover Changes and Their Impacts on Land Surface Temperature in Dhaka, Bangladesh. *Remote Sensing*, **5**, 5969-5998. https://doi.org/10.3390/rs5115969

[12] Cichowicz, R. and Bochenek, A.D. (2024) Assessing the Effects of Urban Heat Islands and Air Pollution on Human Quality of Life. *Anthropocene*, **46**, Article ID: 100433. https://doi.org/10.1016/j.ancene.2024.100433

[13] Wu, Q., Huang, Y., Irga, P., Kumar, P., Li, W., Wei, W., *et al.* (2024) Synergistic Control of Urban Heat Island and Urban Pollution Island Effects Using Green Infrastructure. *Journal of Environmental Management*, **370**, Article ID: 122985. https://doi.org/10.1016/j.jenvman.2024.122985

[14] Rousta, I., Sarif, M.O., Gupta, R.D., Olafsson, H., Ranagalage, M., Murayama, Y., *et al.* (2018) Spatiotemporal Analysis of Land Use/Land Cover and Its Effects on Surface Urban Heat Island Using Landsat Data: A Case Study of Metropolitan City Tehran (1988-2018). *Sustainability*, **10**, Article No. 4433. https://doi.org/10.3390/su10124433

[15] Vohra, R., Kumar, A., Jain, R. and Hemanth, D.J. (2024) Analysis and Prediction of Land Surface Temperature with Increasing Urbanisation Using Satellite Imagery. *Heliyon*, **10**, e40378. https://doi.org/10.1016/j.heliyon.2024.e40378

[16] Rahman, M.R. and Mark, B.G. (2025) Geospatial Analysis of Urban Warming: A Remote Sensing and GIS-Based Investigation of Winter Land Surface Temperature and Biophysical Composition in Rajshahi City, Bangladesh. *Sustainability*, **17**, Article No. 5107. https://doi.org/10.3390/su17115107

[17] Ul Hussan, H., Li, H., Liu, Q., Bashir, B., Hu, T. and Zhong, S. (2024) Investigating Land Cover Changes and Their Impact on Land Surface Temperature in Khyber Pakhtunkhwa, Pakistan. *Sustainability*, **16**, Article No. 2775. https://doi.org/10.3390/su16072775

[18] Regmi, S.R., Thapa, M.S., Adhikari, R. and Regmi, R.R. (2021) Dynamics of Land

Surface Temperature in Response to Land Use Land Cover Change in Phewa Watershed, Kaski, Nepal. *Forestry*: *Journal of Institute of Forestry*, *Nepal*, **18**, 61-80. https://doi.org/10.3126/forestry.v18i01.41758

[19] Kandel, A. and Pokhrel, K. (2024) Study of Urban Sprawl and Its Impact on Vegetation, Land Surface Temperature and Air Pollution Using Remote Sensing and GIS in Kathmandu Valley from 2015 to 2020. *Journal of Geoscience and Environment Protection*, **12**, 28-53. https://doi.org/10.4236/gep.2024.123003

[20] Sarif, M.O., Rimal, B. and Stork, N.E. (2020) Assessment of Changes in Land Use/Land Cover and Land Surface Temperatures and Their Impact on Surface Urban Heat Island Phenomena in the Kathmandu Valley (1988-2018). *ISPRS International Journal of Geo-Information*, **9**, Article No. 726. https://doi.org/10.3390/ijgi9120726

[21] Zhao, W., He, J., Yin, G., Wen, F. and Wu, H. (2019) Spatiotemporal Variability in Land Surface Temperature over the Mountainous Region Affected by the 2008 Wenchuan Earthquake from 2000 to 2017. *Journal of Geophysical Research*: *Atmospheres*, **124**, 1975-1991. https://doi.org/10.1029/2018jd030007

[22] Kc, A., Wagle, N. and Acharya, T.D. (2021) Spatiotemporal Analysis of Land Cover and the Effects on Ecosystem Service Values in Rupandehi, Nepal from 2005 to 2020. *ISPRS International Journal of Geo-Information*, **10**, Article No. 635. https://doi.org/10.3390/ijgi10100635

[23] National Statistical Office, Nepal (2021) National Population and Housing Census 2021.

[24] Zhang, Y., Balzter, H., Liu, B. and Chen, Y. (2017) Analyzing the Impacts of Urbanization and Seasonal Variation on Land Surface Temperature Based on Subpixel Fractional Covers Using Landsat Images. *IEEE Journal of Selected Topics in Applied Earth Observations and Remote Sensing*, **10**, 1344-1356. https://doi.org/10.1109/jstars.2016.2608390

[25] Dissanayake, D., Morimoto, T. and Ranagalage, M. (2019) Accessing the Soil Erosion Rate Based on RUSLE Model for Sustainable Land Use Management: A Case Study of the Kotmale Watershed, Sri Lanka. *Modeling Earth Systems and Environment*, **5**, 291-306. https://doi.org/10.1007/s40808-018-0534-x

[26] Mansourmoghaddam, M., Rousta, I., Ghafarian Malamiri, H., Sadeghnejad, M., Krzyszczak, J. and Ferreira, C.S.S. (2024) Modeling and Estimating the Land Surface Temperature (LST) Using Remote Sensing and Machine Learning (Case Study: Yazd, Iran). *Remote Sensing*, **16**, Article No. 454. https://doi.org/10.3390/rs16030454

[27] Thapa, R.B. and Murayama, Y. (2009) Examining Spatiotemporal Urbanization Patterns in Kathmandu Valley, Nepal: Remote Sensing and Spatial Metrics Approaches. *Remote Sensing*, **1**, 534-556. https://doi.org/10.3390/rs1030534

[28] Scarano, M. and Sobrino, J.A. (2015) On the Relationship between the Sky View Factor and the Land Surface Temperature Derived by Landsat-8 Images in Bari, Italy. *International Journal of Remote Sensing*, **36**, 4820-4835. https://doi.org/10.1080/01431161.2015.1070325

[29] Chowdhury, T.A. and Islam, M.S. (2021) Assessing and Simulating Impacts of Land Use Land Cover Changes on Land Surface Temperature in Mymensingh City, Bangladesh. *Environment and Natural Resources Journal*, **20**, 1-19. https://doi.org/10.32526/ennrj/20/202100110

[30] You, H., Tang, X., Deng, W., Song, H., Wang, Y. and Chen, J. (2022) A Study on the Difference of LULC Classification Results Based on Landsat 8 and Landsat 9 Data. *Sustainability*, **14**, Article No. 13730. https://doi.org/10.3390/su142113730

[31] Guechi, I., Gherraz, H. and Alkama, D. (2021) Correlation Analysis between Biophys-

ical Indices and Land Surface Temperature Using Remote Sensing and GIS in Guelma City (Algeria). *Bulletin de la Société Royale des Sciences de Liège*, **90**, 158-180. https://doi.org/10.25518/0037-9565.10457

[32] Guha, S., Govil, H., Dey, A. and Gill, N. (2018) Analytical Study of Land Surface Temperature with NDVI and NDBI Using Landsat 8 OLI and TIRS Data in Florence and Naples City, Italy. *European Journal of Remote Sensing*, **51**, 667-678. https://doi.org/10.1080/22797254.2018.1474494

[33] Bhuju, U.R., Khadka, M., Neupane, P.K. and Adhikari, R. (1970) A Map Based Inventory of Lakes in Nepal. *Nepal Journal of Science and Technology*, **11**, 173-180. https://doi.org/10.3126/njst.v11i0.4141

[34] Mishra, M. and Sijapati, D.B. (2023) Spatial Distribution of Population in Nepal: On the Basis of 2078 Census. *Journal of Population and Development*, **4**, 68-80. https://doi.org/10.3126/jpd.v4i1.64240

[35] Ali, H.Z. (2021) Estimation of Surface Temperature Using Landsat Satellite Images and Geographic Information Systems for Environmental Studies in Iraq. *Journal of Physics*: *Conference Series*, **1895**, Article ID: 012006. https://doi.org/10.1088/1742-6596/1895/1/012006

[36] Ferrelli, F., Bustos, M.L., Huamantinco-Cisneros, M.A. and Piccolo, M.C. (2015) Utilización de imágenes satelitales para el estudio de la distribución térmica en distintas coberturas del suelo de la ciudad de Bahía Blanca (Argentina). *Revista de Teledetección*, **44**, Article No. 31. https://doi.org/10.4995/raet.2015.4018

[37] Obiefuna, J.N., Okolie, C.J., Nwilo, P.C., Daramola, O.E. and Isiofia, L.C. (2021) Potential Influence of Urban Sprawl and Changing Land Surface Temperature on Outdoor Thermal Comfort in Lagos State, Nigeria. *Quaestiones Geographicae*, **40**, 5-23. https://doi.org/10.2478/quageo-2021-0001

[38] Carlson, T.N. and Ripley, D.A. (1997) On the Relation between NDVI, Fractional Vegetation Cover, and Leaf Area Index. *Remote Sensing of Environment*, **62**, 241-252. https://doi.org/10.1016/s0034-4257(97)00104-1

[39] Nugraha, A.S.A., Kamal, M., Heru Murti, S. and Widyatmanti, W. (2024) Accuracy Assessment of Land Surface Temperature Retrievals from Remote Sensing Imagery: Pixel-Based, Single and Multi-Channel Methods. *Geomatics*, *Natural Hazards and Risk*, **15**, Article ID: 2324975. https://doi.org/10.1080/19475705.2024.2324975

[40] Rakib, A.Al., Akter, K.S., Rahman, N., Arpi, S. and Kafy, A.Al. (2020) Analyzing the Pattern of Land Use Land Cover Change and Its Impact on Land Surface Temperature: A Remote Sensing Approach in Mymensingh, Bangladesh. 1*st International Student Research Conference*, Dhaka, 6 December 2020, 1-11. https://www.academia.edu/download/65116756/NS_09.pdf

[41] Sekertekin, A. and Bonafoni, S. (2020) Sensitivity Analysis and Validation of Daytime and Nighttime Land Surface Temperature Retrievals from Landsat 8 Using Different Algorithms and Emissivity Models. *Remote Sensing*, **12**, Article No. 2776. https://doi.org/10.3390/rs12172776

[42] Xu, D. (2014) Compare NDVI Extracted from Landsat 8 Imagery with That from Landsat 7 Imagery. *American Journal of Remote Sensing*, **2**, Article No. 10. https://doi.org/10.11648/j.ajrs.20140202.11

[43] Kshetri, T.B. (n.d.) NDVI, NDBI and NDWI Calculation Using Land-SAT 7 and 8.

[44] Amini, S., Saber, M., Rabiei-Dastjerdi, H. and Homayouni, S. (2022) Urban Land Use and Land Cover Change Analysis Using Random Forest Classification of Landsat Time Series. *Remote Sensing*, **14**, Article No. 2654. https://doi.org/10.3390/rs14112654

[45] Belgiu, M. and Drăguţ, L. (2016) Random Forest in Remote Sensing: A Review of Applications and Future Directions. *ISPRS Journal of Photogrammetry and Remote Sensing*, **114**, 24-31. https://doi.org/10.1016/j.isprsjprs.2016.01.011

[46] Kasahun, M. and Legesse, A. (2024) Machine Learning for Urban Land Use/Cover Mapping: Comparison of Artificial Neural Network, Random Forest and Support Vector Machine, a Case Study of Dilla Town. *Heliyon*, **10**, e39146. https://doi.org/10.1016/j.heliyon.2024.e39146

[47] Plasse, J. and Adams, N.M. (2019) Multiple Changepoint Detection in Categorical Data Streams. *Statistics and Computing*, **29**, 1109-1125. https://doi.org/10.1007/s11222-019-09858-0

[48] Devkota, P., Dhakal, S., Shrestha, S. and Shrestha, U.B. (2023) Land Use Land Cover Changes in the Major Cities of Nepal from 1990 to 2020. *Environmental and Sustainability Indicators*, **17**, Article ID: 100227. https://doi.org/10.1016/j.indic.2023.100227

[49] Shrestha, S., Poudyal, K.N., Bhattarai, N., Dangi, M.B. and Boland, J.J. (2022) An Assessment of the Impact of Land Use and Land Cover Change on the Degradation of Ecosystem Service Values in Kathmandu Valley Using Remote Sensing and GIS. *Sustainability*, **14**, Article No. 15739. https://doi.org/10.3390/su142315739

[50] Thapa, R.B. and Murayama, Y. (2010) Drivers of Urban Growth in the Kathmandu Valley, Nepal: Examining the Efficacy of the Analytic Hierarchy Process. *Applied Geography*, **30**, 70-83. https://doi.org/10.1016/j.apgeog.2009.10.002

[51] Rimal, B., Zhang, L., Keshtkar, H., Haack, B., Rijal, S. and Zhang, P. (2018) Land Use/Land Cover Dynamics and Modeling of Urban Land Expansion by the Integration of Cellular Automata and Markov Chain. *ISPRS International Journal of Geo-Information*, **7**, Article No. 154. https://doi.org/10.3390/ijgi7040154

[52] Deilami, K., Kamruzzaman, M. and Liu, Y. (2018) Urban Heat Island Effect: A Systematic Review of Spatio-Temporal Factors, Data, Methods, and Mitigation Measures. *International Journal of Applied Earth Observation and Geoinformation*, **67**, 30-42. https://doi.org/10.1016/j.jag.2017.12.009

[53] Yang, L., Qian, F., Song, D. and Zheng, K. (2016) Research on Urban Heat-Island Effect. *Procedia Engineering*, **169**, 11-18. https://doi.org/10.1016/j.proeng.2016.10.002

[54] Bhandari, S. and Zhang, C. (2022) Urban Green Space Prioritization to Mitigate Air Pollution and the Urban Heat Island Effect in Kathmandu Metropolitan City, Nepal. *Land*, **11**, Article No. 2074. https://doi.org/10.3390/land11112074

[55] Jamarkattel, U., Lamichhane, B.R., Gautam, S., K.C., N., Sherchan, B. and Horanont, T. (2025) Analyzing Urban Heat Islands in Pokhara Metropolitan City-Nepal through Remote Sensing Techniques. *Remote Sensing Applications: Society and Environment*, **37**, Article ID: 101479. https://doi.org/10.1016/j.rsase.2025.101479

[56] Karunaratne, S., Athukorala, D., Murayama, Y. and Morimoto, T. (2022) Assessing Surface Urban Heat Island Related to Land Use/Land Cover Composition and Pattern in the Temperate Mountain Valley City of Kathmandu, Nepal. *Remote Sensing*, **14**, Article No. 4047. https://doi.org/10.3390/rs14164047

[57] Pandey, H.P., Maraseni, T.N., Apan, A., Pokhrel, S. and Zhang, H. (2025) Lessons from a Participatory Forest Restoration Program on Socio-Ecological and Environmental Aspects in Nepal. *Trees, Forests and People*, **20**, Article ID: 100854. https://doi.org/10.1016/j.tfp.2025.100854

[58] Gautam, A.P., Shivakoti, G.P. and Webb, E.L. (2004) Forest Cover Change, Physiography, Local Economy, and Institutions in a Mountain Watershed in Nepal. *Environmental Management*, **33**, 48-61. https://doi.org/10.1007/s00267-003-0031-4

[59] Karakuş, C.B. (2019) The Impact of Land Use/Land Cover (LULC) Changes on Land

Surface Temperature in Sivas City Center and Its Surroundings and Assessment of Urban Heat Island. *Asia-Pacific Journal of Atmospheric Sciences*, **55**, 669-684. https://doi.org/10.1007/s13143-019-00109-w

[60] Gurung, S., Singh, S.K., Bhattarai, S. and Agriculture, B. (n.d.) Study the Status of Fish Farming in Shiktahan VDC of Rupandehi District of Nepal.

[61] Wang, Q., Peng, K., Tang, Y., Tong, X. and Atkinson, P.M. (2021) Blocks-Removed Spatial Unmixing for Downscaling MODIS Images. *Remote Sensing of Environment*, **256**, Article ID: 112325. https://doi.org/10.1016/j.rse.2021.112325